https://doi.org/10.51483/IJAIML.6.1.2026.102-117 ISSN: 2789-2557

SvedbergOpen
DISSEMINATION OF KNOWLEDGE

International Journal of Artificial Intelligence and Machine Learning

Publisher's Home Page: https://www.svedbergopen.com/

Research Paper Open Access

Multi-Year Flood Inundation Modelling in Kolhapur, India Using SAR Observations and Machine Learning

Shrikant Kate[1*] and Vidula Swami[2]

[1]Research Scholar, Department of Technology, Shivaji University, Kolhapur 416004, India. E-mail: srk.rs.dot@unishivaji.ac.in

[2]Professor (Former), Department of Civil Engineering, KIT's College of Engineering (Autonomous), Kolhapur 416234, India. E-mail: vidulaswami@gmail.com

Article Info

Volume 6, Issue 1, January 2026
Received : 10 September 2025
Accepted : 28 November 2025
Published : 20 January 2026
doi: 10.51483/IJAIML.6.1.2026.102-117

Abstract

Flood forecasting in monsoon-dominated river basins is challenged by sparse hydrological observations, rapid urban expansion, and strong seasonal variability. This study presents a multi-year machine-learning framework (2017-2025) that integrates Sentinel-1 SAR flood extents, CHIRPS and IMD rainfall, ERA5-Land hydrometeorological variables, and SRTM-derived physiographic attributes to predict flood inundation in Kolhapur, India. Random Forest (RF), Support Vector Machine (SVM), and Multi-Layer Perceptron (MLP) models were trained using progressively expanding temporal windows to evaluate the effect of multi-year hydroclimatic diversity on predictive skill. RF consistently achieved the highest accuracy and spatial coherence, with strong generalization to the independently withheld 2025 flood event. The multi-year approach captures monsoon variability-including extreme floods, prolonged wet spells, and deficit rainfall years-allowing the models to learn interannual rainfall-runoff-inundation relationships. Antecedent hydrological indicators such as cumulative rainfall, runoff, and soil moisture were identified as key predictors enabling short-range flood forecasting before inundation occurs. Beyond the local case study, the workflow demonstrates strong transferability to other monsoon-affected and data-scarce basins because it relies on globally available satellite datasets, terrain-based predictors, and non-parametric ML algorithms. The methodology is operationally scalable and adaptable for flood early-warning systems in rapidly urbanizing river basins worldwide.

Keywords: *Flood inundation mapping, Machine learning, Synthetic Aperture Radar (SAR), Hydrometeorological modelling, Urban flood forecasting*

1. Introduction

Flooding remains one of the most disruptive hydro-meteorological hazards, repeatedly affecting social,

* *Corresponding author: Shrikant Kate, Research Scholar, Department of Technology, Shivaji University, Kolhapur 416004, India. E-mail: srk.rs.dot@unishivaji.ac.in*

economic, and infrastructural systems. These impacts are intensified in monsoon-dominated regions where sharp rainfall variability, expanding urban footprints, and insufficient drainage capacity heighten flood susceptibility (Ganjirad and Delavar, 2023). In many such areas, conventional hydrological monitoring networks are sparse or inconsistent, limiting their ability to capture the rapid onset and spatial evolution of flood events. This limitation has increased reliance on remote-sensing technologies and data-driven modelling approaches, which provide scalable and timely means of characterizing flood processes in complex, data-scarce urban environments.

Synthetic Aperture Radar (SAR) has emerged as a critical tool for monsoon-season flood assessment because it can acquire data through cloud cover and low-light conditions, precisely when surface observations are most needed (Iselborn *et al.*, 2023). Sentinel-1 SAR, with its C-band VV/VH polarization, is particularly effective, as water surfaces exhibit distinct backscatter attenuation that supports reliable inundation mapping even during prolonged cloudy periods (Singha and Swain, 2022). When SAR observations are combined with terrain parameters, land-use/land-cover information, soil characteristics, drainage geometry, and hydrometeorological variables such as rainfall, runoff, and soil moisture, they form a comprehensive predictor space capable of representing the physical controls governing flood dynamics (Ganjirad and Delavar, 2023; Ho and Mostafavi, 2025).

Machine-Learning (ML) techniques have demonstrated strong utility for flood mapping and susceptibility modelling, especially when applied to multi-sensor datasets. Studies have shown that models such as Random Forest (RF) and Support Vector Machine (SVM) can accurately characterize flood extents across heterogeneous landscapes. For example, ML models using fused Sentinel-1 and Sentinel-2 data effectively delineated flood extents during the 2021 Gediz Plain flood (Iselborn *et al.*, 2023). Similar advancements in Iran demonstrated that integrating SAR-derived inventories with Support Vector Regression (SVR) improved susceptibility prediction by representing terrain and rainfall-driven factors (Ganjirad and Delavar, 2023). Additional evidence from Tropical Storm Imelda further supports the capability of ML–SAR fusion, with patch-level RF classification exceeding 94% accuracy (Ho and Mostafavi, 2025).

Building on these advancements, the present study develops a multi-model flood prediction framework for Kolhapur City using RF, SVM, and Multi-Layer Perceptron (MLP) classifiers. The framework integrates a multi-year database (2017-2024) consisting of Sentinel-1 flood maps, CHIRPS and IMD rainfall, ERA5-Land hydrological fields, and terrain metrics derived from SRTM DEM. Missing SAR years (2019, 2024) were reconstructed using DEM-based water-spread modelling and rainfall accumulation analysis. Predictor variables—including rainfall, runoff, elevation, slope, aspect, soil type, drainage density, and LULC—capture dominant physiographic and hydroclimatic controls (Tehrany *et al.*, 2014; Sanyal and Lu, 2004; Mosavi *et al.*, 2020; Manfreda *et al.*, 2018).

Models were trained using stratified samples from 2017-2024 and validated independently on 2025. Accuracy metrics and Taylor-diagram diagnostics jointly evaluated model correlation, variance representation, and error behavior. Results demonstrate that fusing multi-source geospatial datasets with ML significantly enhances flood-prediction reliability in monsoon-affected, data-limited regions like Kolhapur, supporting improved early-warning and risk-management strategies.

2. Study Area

Kolhapur City, located in southwestern Maharashtra within the Panchganga River basin (17.3°-17.5° N, 74.2°-74.4° E), experiences a tropical monsoonal climate with 1,100-1,200 mm of annual rainfall, concentrated from June to September (IMD, 2022). Figure 1 shows the study area. The region consists of gently sloping alluvial plains and low basaltic uplands linked to the Deccan Traps (CGWB, 2019). Rapid urban growth has expanded impervious surfaces, increasing runoff and flood vulnerability during intense monsoon events (Sharma *et al.*, 2021). Flooding is driven by rainfall–runoff dynamics and worsened by inadequate drainage and floodplain encroachment (Dey *et al.*, 2022). These combined physiographic and urban pressures make Kolhapur an appropriate setting for evaluating monsoon-induced urban flooding using remote sensing and machine-learning frameworks (Sanyal and Lu, 2004; Manfreda *et al.*, 2018).

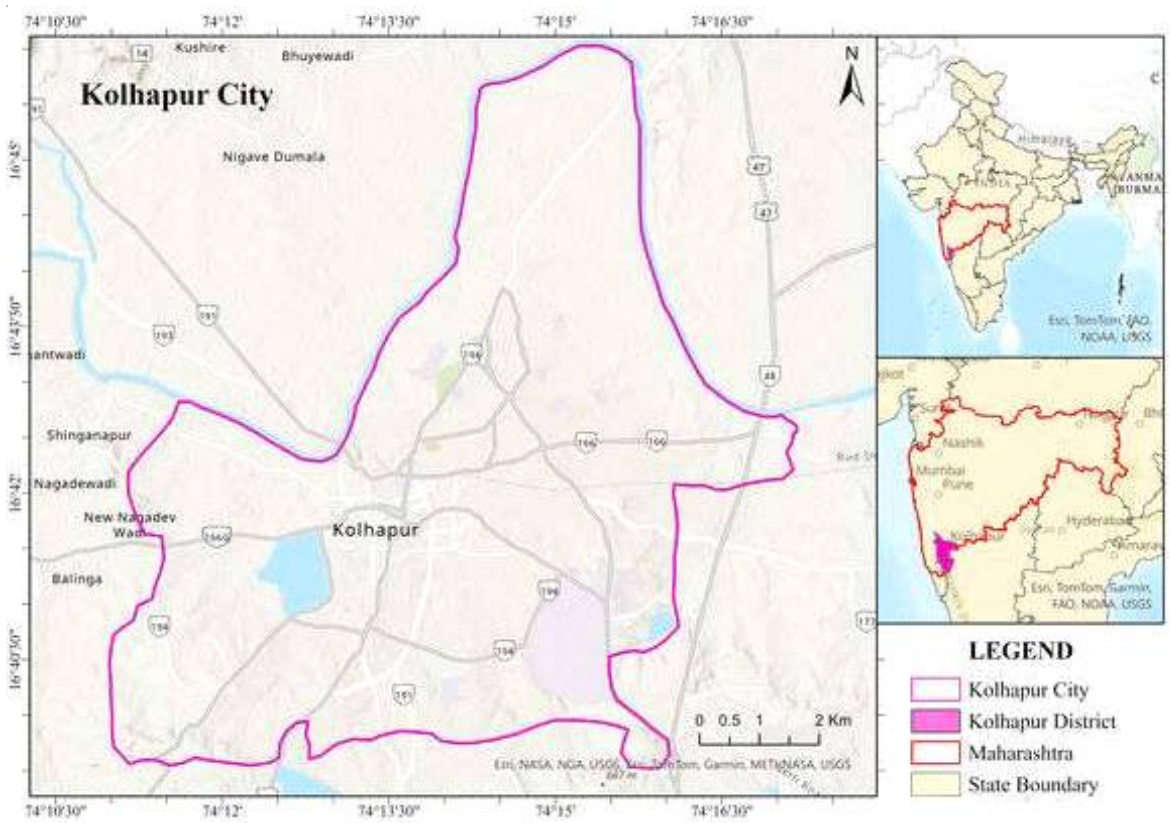

Figure 1: Study Area

3. Data Structure and Predictors

A multi-source geospatial data architecture was developed to generate predictor variables for flood-inundation modelling. Rainfall inputs were obtained from CHIRPS daily precipitation data, refined with India Meteorological Department (IMD) observations to capture localized monsoon variability often missed by satellite-only products (Funk *et al.*, 2015; IMD, 2022). Hydrometeorological variables—surface runoff, soil moisture, and land–atmosphere fluxes—were sourced from ERA5-Land, which provides physically consistent, sub-daily reanalysis fields through advanced data assimilation (Muñoz-Sabater *et al.*, 2021). This integration enables representation of both large-scale monsoon processes and fine-scale catchment responses.

Flood-inundation information was derived from Sentinel-1 GRD SAR imagery, whose C-band signal supports reliable monsoon-season flood detection. For years with missing SAR coverage, inundation was reconstructed using DEM-constrained rainfall-accumulation modelling. Physiographic variables, including elevation, slope, and aspect, were extracted from the 30-m SRTM DEM, while soil and LULC data were obtained

Table 1: Data Used for Flood Prediction Model

Data Type	Dataset Name	Source	Resolution	Temporal Coverage
Rainfall	CHIRPS Daily	UCSB-CHG	0.05°	2017–2025
Runoff	ERA5-Land Monthly-by-Hour	ECMWF Copernicus	0.1°	2017–2025
Flood Inundation (SAR)	Sentinel-1 GRD	ESA Copernicus	10 m	2017–2025
Land Use/Land Cover	Sentinel LULC	ESA	10 m	
Elevation	SRTM DEM	USGS	30 m	2014
Soil Type	FAO Soil Dataset	FAO/ISRIC		

from FAO/ISRIC and ESA products. Collectively, these datasets provide a harmonized depiction of terrain and hydroclimatic controls for 2017-2025.

Table 1 provides detailed information on the data used for the flood prediction model. A flood-inundation point database was generated by sampling all raster predictors for 2017-2025, with each point assigned a binary label (flooded/non-flooded) derived from SAR-based masks or DEM–rainfall reconstructions. Predictor variables included rainfall, runoff, elevation, slope, aspect, soil type, drainage density, and LULC; IMD station rainfall was converted to a 15-day moving average to represent event-scale precipitation (IMD, 2022). Inundation extents were mapped using Sentinel-1 VV-polarized backscatter, processed through median filtering and regionally calibrated thresholding (–12 to –18 dB), a robust method for monsoon flood detection (Shen *et al.*, 2019; Twele *et al.*, 2016). Years lacking adequate SAR coverage (2019, 2024) were reconstructed using rainfall-accumulation modelling constrained by DEM topography, ensuring continuity across the study period (Amitrano *et al.*, 2020). All predictors were resampled to 30 m resolution and normalized using min-max scaling. Data from 2017-2024 were used for ML model training, while 2025 was withheld for independent forecasting evaluation. Figure 2 shows the Flow chart for Machine-learning based flood prediction model.

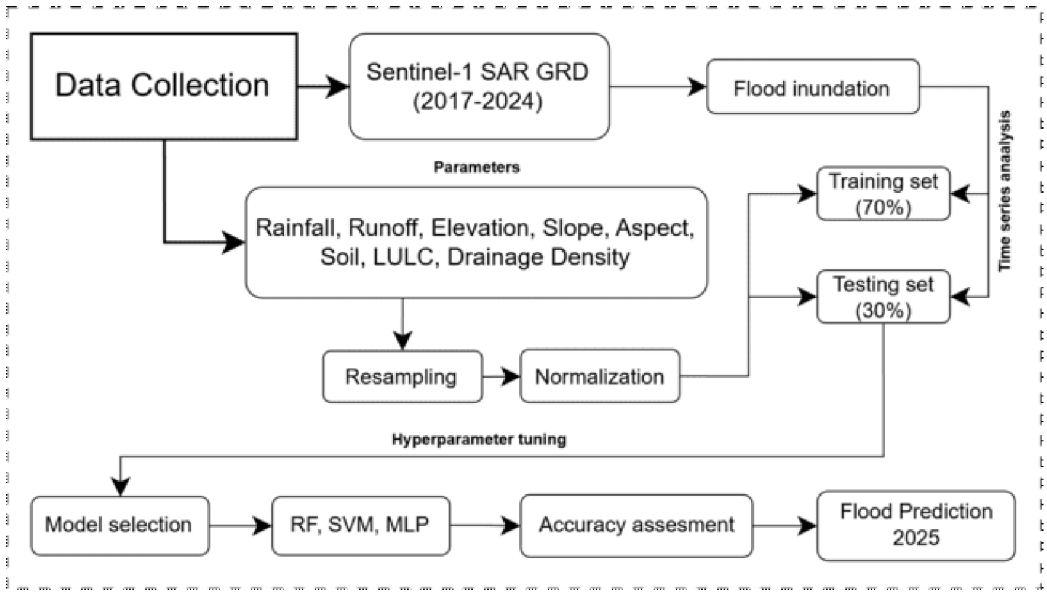

Figure 2: Flow Chart for Machine-Learning Based Flood Prediction Model

3.1. Cumulative Time-Progressive Training Design

A cumulative modelling scheme was employed to quantify how progressively increasing temporal information influences classification skill. For each terminal year Y Î [2017, 2024], the training corpus comprised all samples satisfying

Year Î [2017, Y] ....(1)

Yielding eight incremental training windows: 2017; 2017-2018; …; 2017-2024. Within each window, pooled observations were split into 70% training and 30% internal testing subsets using stratified sampling to maintain the class ratio between inundated and non-inundated instances. The complete 2025 dataset was reserved exclusively for out-of-sample evaluation and was not included in any internal partitioning.

3.2. Algorithms and Implementation

Three commonly used supervised classifiers were evaluated: Random Forest (RF), Support Vector Machine (SVM), and Multi-Layer Perceptron (MLP).

RF is an ensemble approach that aggregates predictions from a large number of decision trees grown on bootstrapped samples and randomly selected feature subsets (Breiman, 2001). For an ensemble of T trees with predictions $h_t(x)$, the final class is which reduces variance and increases robustness in classification.

$$\hat{y} = \text{mode}\left\{h_1(x), h_2(x), \ldots, h_T(x)\right\} \quad \ldots(2)$$

SVM constructs a maximal-margin separating hyperplane (Cortes and Vapnik, 1995). The classifier takes the form subject to margin maximization, while nonlinear boundaries are introduced through kernel functions $K(x_i, x_j)$ that implicitly map data into a higher-dimensional feature space.

$$f(x) = w^T x + b \quad \ldots(3)$$

MLP is a feed-forward neural network trained with back-propagation (Rumelhart *et al.*, 1986). Each hidden layer performs allowing the network to capture complex nonlinear predictor–response relationships.

$$h^{(l)} = \sigma\left(W^{(l)} h^{(l-1)} + b^{(l)}\right) \quad \ldots(4)$$

All models were implemented in Python using the scikit-learn library, which provides unified interfaces for classification, preprocessing, tuning, and evaluation (Pedregosa *et al.*, 2011).

3.3. Pre-Processing and Model Pipelines

RF was trained on the raw predictor values because decision-tree ensembles are invariant to monotonic feature transformations, and splitting rules depend only on threshold ordering rather than absolute magnitudes (Breiman, 2001). In contrast, SVM and MLP are sensitive to differences in feature scale; therefore, all continuous predictors were standardized using where μ and σ denote the feature-wise mean and standard deviation. Standardization was implemented with StandardScaler, and all pre-processing and model-fitting steps were encapsulated within Pipeline objects to guarantee identical transformations during both training and prediction (Pedregosa *et al.*, 2011).

$$z = \frac{x - \mu}{\sigma} \quad \ldots(5)$$

Hyperparameter optimization was conducted through a combination of structured grid search and iterative heuristic refinement, with the objective of improving class separability, stabilizing gradient-based learning, and strengthening temporal generalization across monsoon years exhibiting substantial hydroclimatic variability. This multistage tuning process emphasized parameter configurations that delivered consistent predictive skill while maintaining computational efficiency, a balance that is particularly important for operational modelling frameworks (Bergstra and Bengio, 2012; Pedregosa *et al.*, 2011). Such an approach

Table 2: Hyperparameter tuning Used for RF, SVM, and MLP models in flood inundation prediction

Model	Hyperparameters
Random Forest (RF)	• Number of trees: 1000 • Maximum depth: 12 • Minimum samples split: 6 • Minimum samples per leaf: 3 • Feature selection: log2 • Class weight: balanced subsample • Bootstrap: Enabled
Support Vector Machine (SVM)	• Kernel: Radial Basis Function (RBF) • C: 2 • Gamma: scale • Class weight: balanced
Multi-Layer Perceptron (MLP)	• Hidden layers: 128, 64 • Activation: ReLU • Optimizer: Adam • L2 regularization (α): 5×10^{-4} • Max iterations: 500

aligns with established guidance in hydrological machine-learning applications, where careful hyperparameter selection is essential to mitigate overfitting, enhance robustness under non-stationary conditions, and ensure reliable performance when models encounter previously unseen rainfall-runoff regimes (Mosavi *et al.*, 2018). Table 2 presents the hyperparameter tuning used for RF, SVM, and MLP models in flood inundation prediction.

3.4. Evaluation Protocol

For each cumulative end year Y, the workflow followed a three-step procedure for RF, SVM, and MLP. First, models were trained on a 70% stratified subset from 2017-Y, preserving the flooded/non-flooded class balance. Second, predictive skill was assessed on the remaining 30% internal test data using accuracy. Third, models were applied to the independent 2025 dataset to evaluate temporal transferability. Internal and external accuracies were plotted against cumulative years, supported by Taylor-diagram and confusion-matrix diagnostics (Willmott *et al.*, 2012; Taylor, 2001). These evaluations identified the most robust classifier for operational flood prediction in monsoon-affected, data-limited regions (Mosavi *et al.*, 2020; Khosravi *et al.*, 2018).

4. Findings and Discussion

4.1. Rainfall Dynamics and Spatiotemporal Flood Inundation Patterns

Rainfall analysis from the IMD Kolhapur station shows strong intra-monsoon variability during 2017-2025, with peak intensities between mid-July and late August, consistent with Southwest Monsoon behavior (Gadgil, 2018). A 15-day moving average highlighted rainfall-accumulation phases linked to flood onset, which corresponded closely with Sentinel-1 SAR-derived inundation patterns. Figure 3 shows the daily rainfall, 15-day moving average rainfall for 2017-2025 at Kolhapur. This alignment reinforces the established role of cumulative precipitation and antecedent wetness in driving floods in saturation-prone urban catchments (Sharma *et al.*, 2021; Sanyal and Lu, 2004).

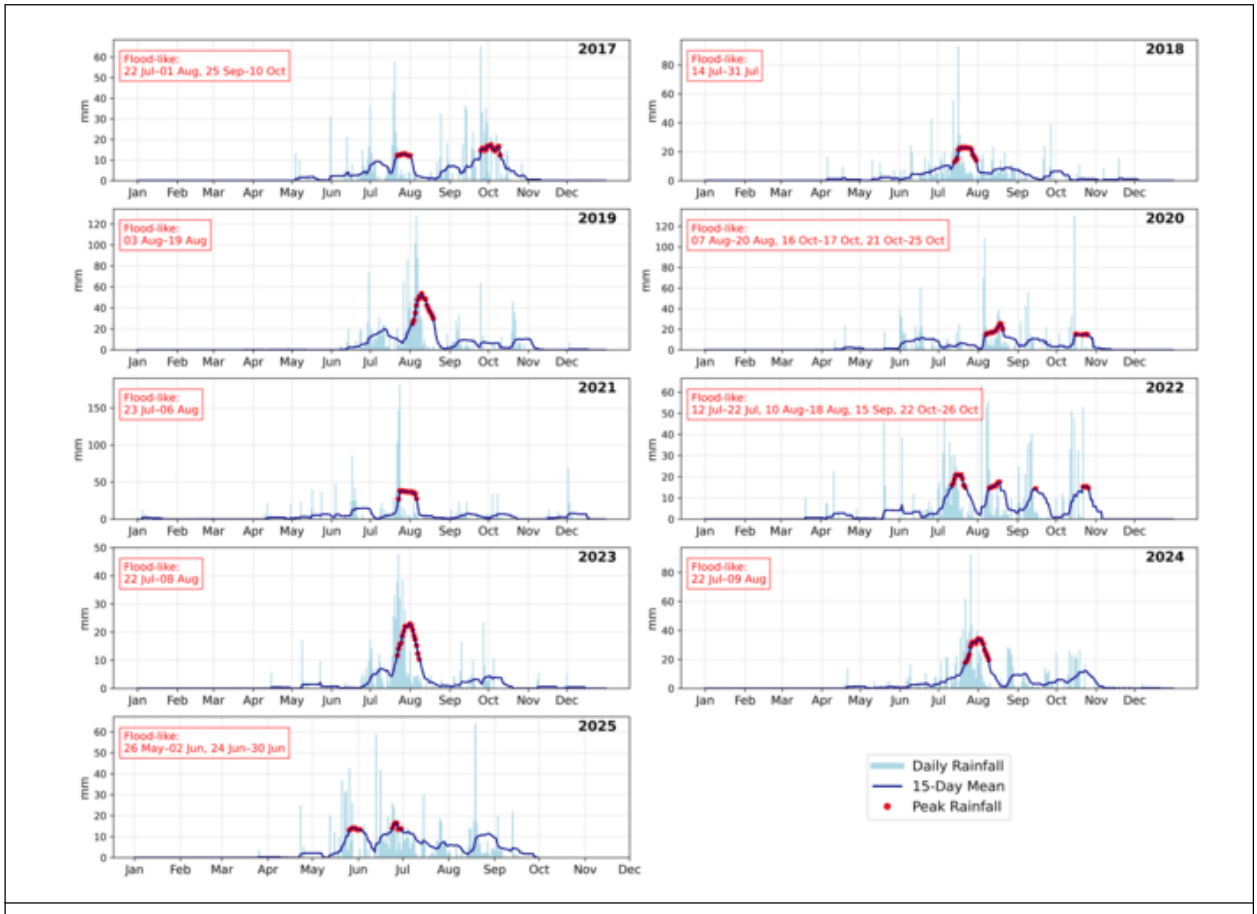

Figure 3: Daily Rainfall, 15-Day Moving Average Rainfall for 2017-2025 at Kolhapur. Red-Highlighted Windows Indicate Flood-Like Rainfall Periods Using IMD Station Data

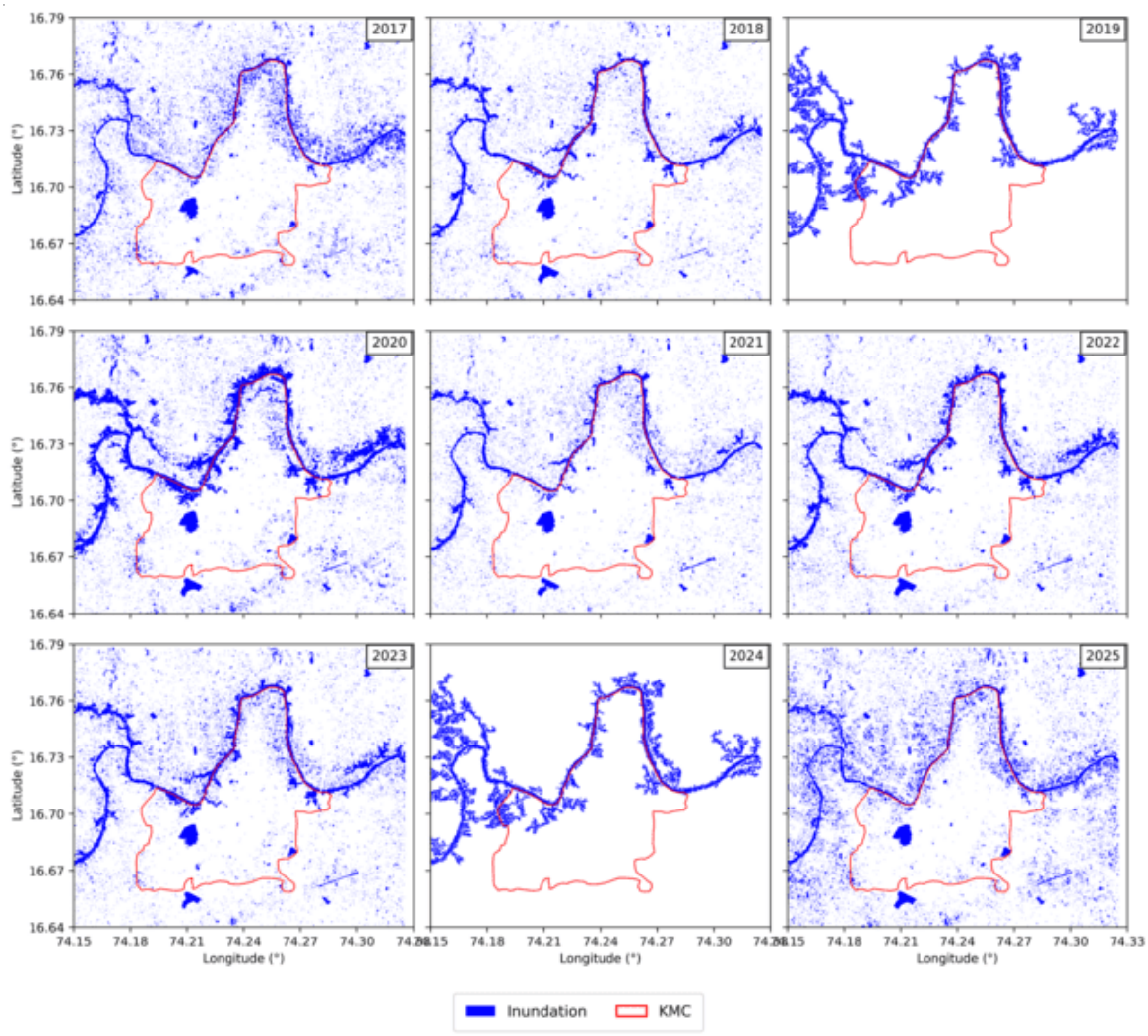

Figure 4: Multi-Year Inundation Extent for 2017-2025 within the Kolhapur City Derived from Sentinel-1 SAR, Flood Clusters along the Panchganga River and Adjacent Low-Elevation Zones

Rainfall characteristics varied across years: prolonged multi-pulse events in 2017, 2020, 2021, and 2022 sustained wetness and extended inundation, while 2019 featured fewer but intense convective bursts, illustrating the influence of short-duration extremes (Houze *et al.*, 2017). The 2025 monsoon showed two major accumulation phases that matched predicted flood extents, further confirming cumulative rainfall as a primary flood driver (Dey *et al.*, 2022; Rodríguez-Blanco *et al.*, 2012).

Figure 4 shows Multi-year inundation extent for 2017-2025 within the Kolhapur city derived from Sentinel-1 SAR, flood clusters along the Panchganga River and adjacent low-elevation zones. Red-highlighted windows indicate flood-like rainfall periods using IMD station data. The 2025 inundation map produced by RF, MLP, and SVM effectively reproduced known flood hotspots and terrain-controlled pathways, aligning with SAR-based studies (Pham *et al.*, 2020; Manfreda *et al.*, 2018) and established geomorphological controls (Tehrany *et al.*, 2014; Khosravi *et al.*, 2018), demonstrating strong applicability for monsoon-season early warning. Figure 5 shows Cumulative model accuracy (2017-2024) showing performance improvements, with Random Forest performing best, followed by SVM and MLP.

4.2. Model Performance and Feature Importance Analysis

Comparative evaluation of Random Forest (RF), Support Vector Machine (SVM), and Multilayer Perceptron (MLP) across cumulative training periods (2017-2024) shows clear differences in flood-prediction skill for Kolhapur. RF consistently achieved the highest accuracies (0.75-0.80), reflecting the strength of ensemble tree methods in capturing nonlinear hydrometeorological interactions (Breiman, 2001; Choubin *et al.*, 2019). SVM

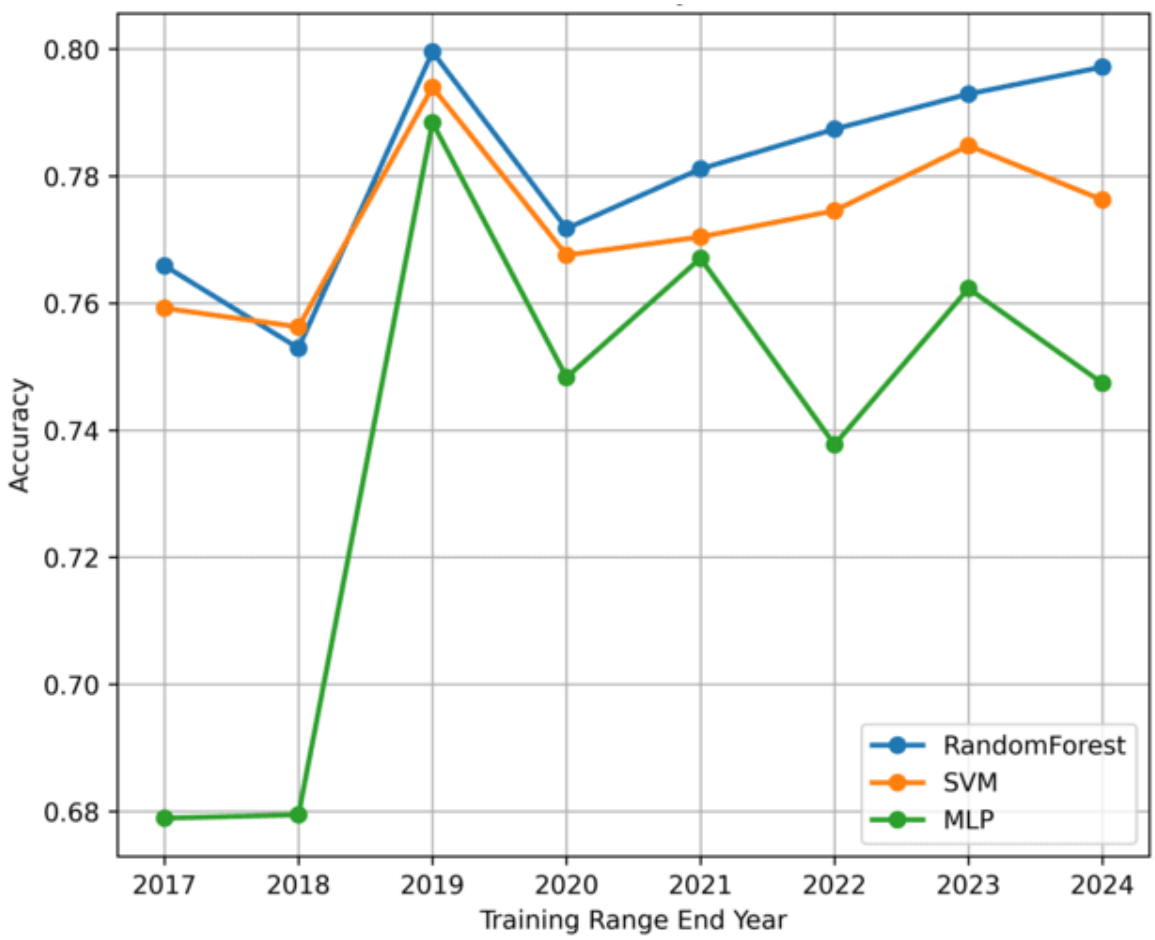

Figure 5: Cumulative Model Accuracy (2017-2024) Showing Performance Improvements, with Random Forest Performing Best, Followed by SVM and MLP

Table 3: Performance of RF, SVM, and MLP Models Using Testing Data (2017-2024)

Model	Accuracy	Precision	Recall	F1 Score	RMSE
Random Forest	0.797156	0.799066	0.797038	0.796786	0.450382
SVM	0.776244	0.776273	0.776258	0.776243	0.473028
MLP	0.747386	0.747409	0.747399	0.747385	0.502607

performed steadily (0.75-0.79), aligning with its established robustness in high-dimensional remote-sensing applications (Mountrakis *et al.*, 2011; Tehrany *et al.*, 2014).

Using the full 2017-2024 dataset, RF attained the highest accuracy (0.797) with strong precision-recall behavior, whereas SVM achieved moderate accuracy (0.776). MLP performed worst (0.747), reflecting challenges in modelling complex geospatial relationships without extensive tuning. Overall, RF demonstrated the strongest generalization, supporting its selection for predicting 2025 flood extent.

Table 3 presents the performance of RF, SVM, and MLP models using testing data (2017-2024). Although the MLP showed gradual performance gains as additional multi-year training data were incorporated, its predictive skill consistently remained below that of the RF and SVM models. This behavior is consistent with findings reported in the hydrological modelling literature, where neural network architectures often face challenges related to convergence instability, sensitivity to noisy or sparse predictor fields, and difficulty in learning from imbalanced datasets that characterize flood-non-flood distributions (Mosavi *et al.*, 2018). These limitations can hinder the MLP's ability to capture complex hydrometeorological interactions without extensive

tuning or large, high-quality training datasets, which likely contributed to its comparatively weaker performance in this study.

Permutation-based feature importance (Figure 6) shows that elevation, LULC, runoff, drainage density, and rainfall were the dominant predictors across all models. Elevation ranked highest, reflecting its key control on flow direction, accumulation zones, and flood propagation in low-lying monsoon-fed basins (Tehrany *et al.*, 2014; Sanyal and Lu, 2004). LULC was also critical, capturing the influence of urban expansion and impervious surface growth on runoff responses in rapidly developing Indian cities (Sharma *et al.*, 2021). Hydrometeorological factors—particularly cumulative rainfall and runoff—were major contributors, consistent with the role of multi-day precipitation and antecedent wetness in driving monsoon-region floods (Rodríguez-Blanco *et al.*, 2012; Houze *et al.*, 2017). These results emphasize the combined influence of terrain, land-use change, and monsoon rainfall in shaping inundation patterns in Kolhapur.

The Random Forest (RF) classifier showed the highest predictive reliability for operational flood forecasting in Kolhapur. Its feature importance patterns indicate that RF effectively captures key physical and geomorphic controls on inundation, including terrain, drainage structure, and monsoon-driven hydrometeorological forcing. This performance is consistent with prior studies demonstrating the strength of ensemble tree models in representing nonlinear interactions in complex urban-riverine systems (Choubin *et al.*, 2019; Khosravi *et al.*, 2018). Overall, RF provides a robust basis for flood early-warning and risk-management applications in monsoon-affected urban catchments.

4.3. Model Performance of Ensemble for Flood Prediction

Model evaluation using the 2017-2024 training dataset clearly differentiates the predictive skill of RF, SVM, and MLP for forecasting the 2025 flood event. The Taylor diagram (Figure 7) shows that RF aligns most closely with observed inundation, achieving the highest correlation (0.48) and lowest centred RMSE (0.51). SVM performs moderately (CORR = 0.46; CRMS = 0.52), while MLP exhibits weaker agreement (CORR = 0.40; CRMS = 0.55). All models maintain standard deviations near the observed (~0.50), indicating adequate representation of overall flood variability (Willmott *et al.*, 2012; Taylor, 2001; Khosravi *et al.*, 2018). These findings confirm RF's superior predictive consistency under monsoon-driven flood conditions.

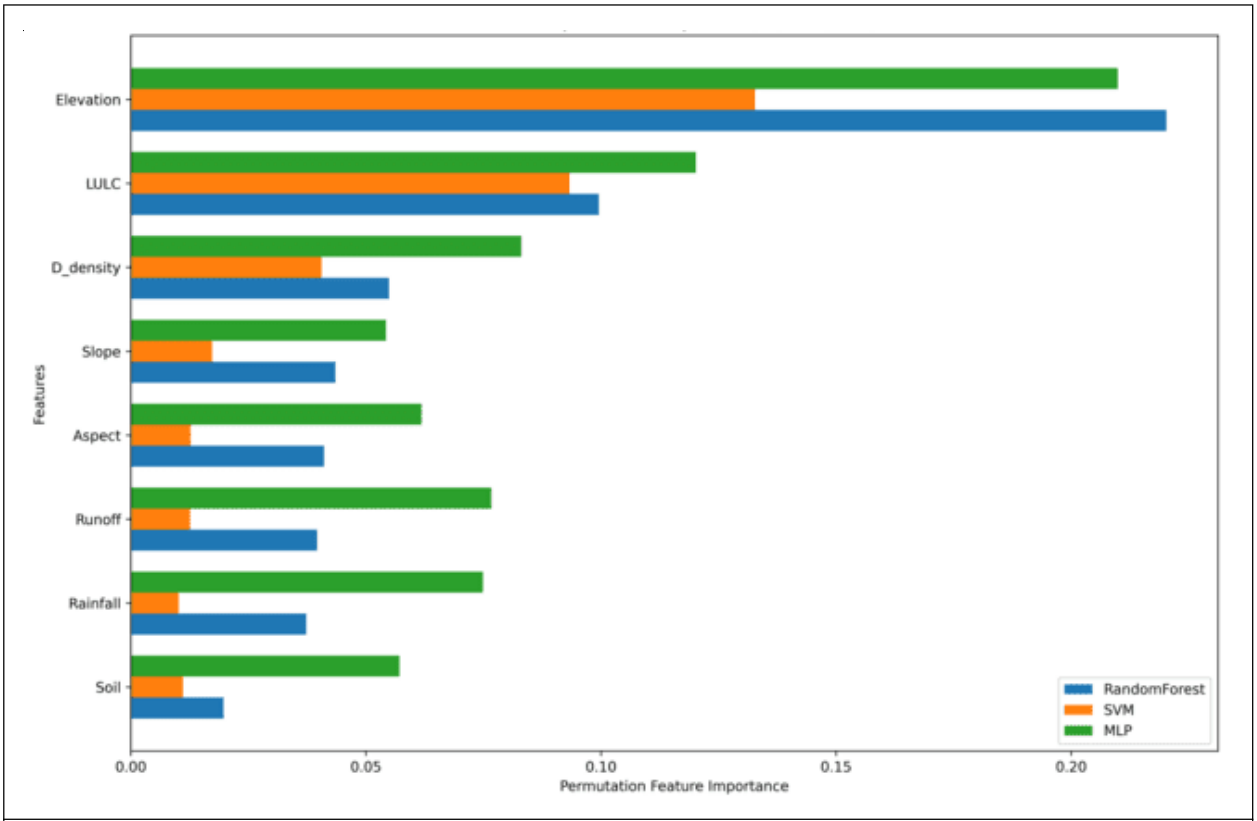

Figure 6: Permutation Feature Importance for the Random Forest, SVM, and MLP Models

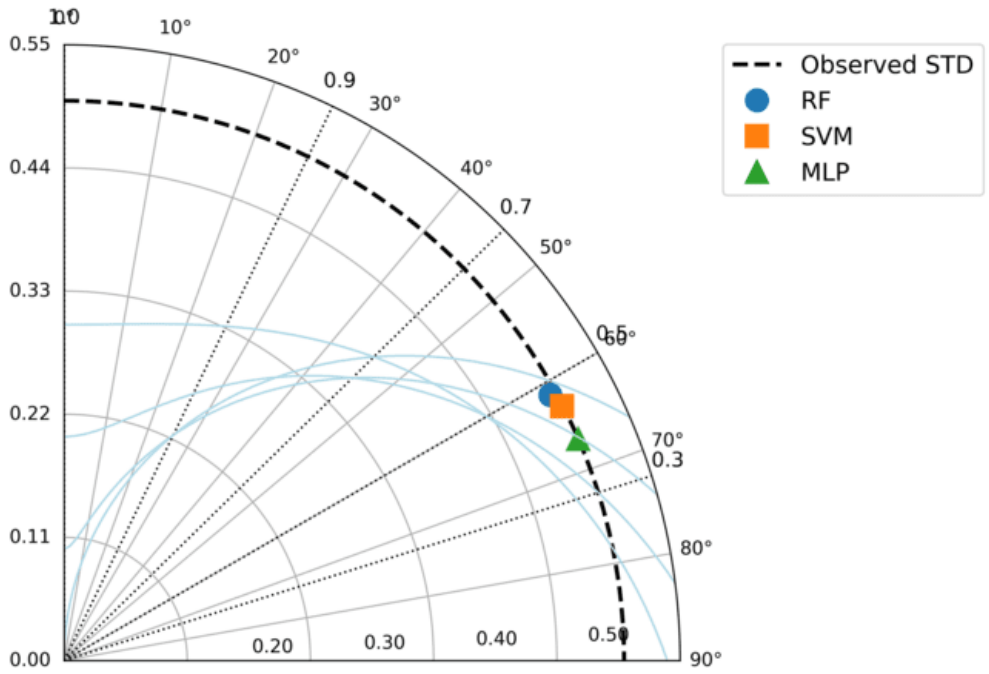

Figure 7: Taylor Diagram Comparing RF, SVM, and MLP against Observations. RF Shows the Closest Match to the Reference Standard Deviation and Highest Correlation, Followed by SVM and MLP

The confusion matrices (Figure 8) highlight clear differences in model behavior for flood-non-flood classification. Random Forest (RF) shows the most balanced performance, correctly detecting 902 flooded and 1,004 non-flooded pixels, resulting in the lowest misclassification. Support Vector Machine (SVM) identifies more true positives (931) but generates a higher number of false positives (274), a common outcome for margin-based classifiers in imbalanced hydrological datasets (Mountrakis *et al.*, 2011; Choubin *et al.*, 2019). Multilayer Perceptron (MLP) exhibits the most confusion, with 308 false positives and 296 false negatives, reflecting neural networks' sensitivity to hyperparameters, non-convex optimization, and noisy geospatial inputs (Abadi *et al.*, 2016). Overall, RF demonstrates superior stability and discrimination compared to SVM and MLP for monsoon-driven flood classification.

The Random Forest (RF) model provides the most reliable prediction of the 2025 flood scenario, aligning with evidence that ensemble tree methods often outperform kernel-based and neural models in flood susceptibility and hydrological forecasting due to their robustness to noisy inputs, limited hyperparameter sensitivity, and ability to capture complex nonlinear relationships (Tehrany *et al.*, 2014; Mosavi *et al.*, 2020). RF's superior performance indicates that it more effectively represents key geomorphological and hydrometeorological controls—such as terrain, drainage structure, and monsoon rainfall dynamics—than SVM or MLP. This behavior is consistent with studies demonstrating RF's strong generalization in

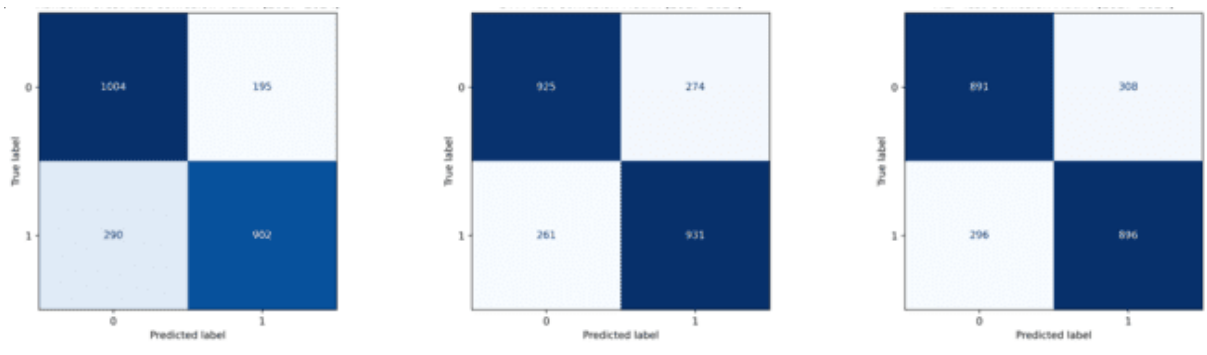

Figure 8: a) Random Forest, b) SVM, and c) MLP Confusion Matrices for Test Data (2017-2024)

environmentally heterogeneous and hydroclimatically variable regions (Khosravi *et al.*, 2018; Choubin *et al.*, 2019).

4.4. Model Evaluation and 2025 Binary Flood Prediction

Binary flood prediction models trained on the 2017-2024 hydrometeorological dataset were applied to classify 2025 flood conditions. The confusion matrices (Figure 9) indicate that Random Forest (RF) performed best, correctly identifying the highest number of flooded (TP = 323) and non-flooded (TN = 411) pixels, with the lowest false positives and false negatives. SVM achieved moderate accuracy, while MLP showed higher misclassification, particularly along flood boundaries under variable monsoon conditions. This performance pattern aligns with studies showing RF's superiority in binary flood detection due to its robustness to noisy inputs, high-dimensional predictors, and nonlinear hydrometeorological interactions (Khosravi *et al.*, 2018; Mosavi *et al.*, 2020; Pham *et al.*, 2020). Overall, RF remains the most reliable operational classifier for monsoon-driven inundation prediction in data-scarce urban river basins.

The year-wise training window experiment (2017-2024) highlights how additional monsoon seasons improve model generalization (Figure 10). When trained only on 2017 data, forecasting skill for 2025 was limited: RF achieved 66.40%, SVM 49.70%, and MLP 49.50%. Accuracy increased markedly as more years were added, demonstrating the value of learning from varied rainfall intensity, antecedent moisture, and runoff conditions that shape flood-non-flood transitions in monsoon systems (Janizadeh *et al.*, 2019; Mosavi *et al.*, 2020). RF remained the strongest performer, reaching 73.84%, while SVM improved to 72.94% and MLP to 68.21%, though still less effective.

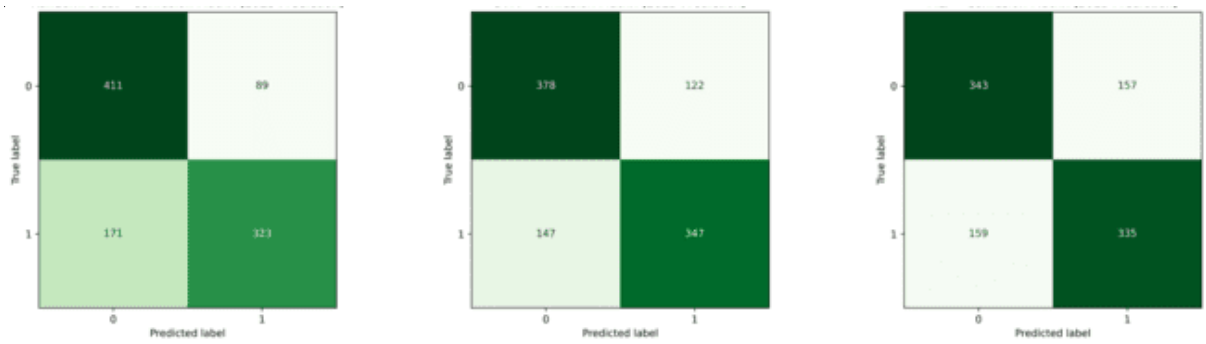

Figure 9: a) Random Forest, b) SVM, and c) MLP Confusion Matrices for Predicted Data (2025)

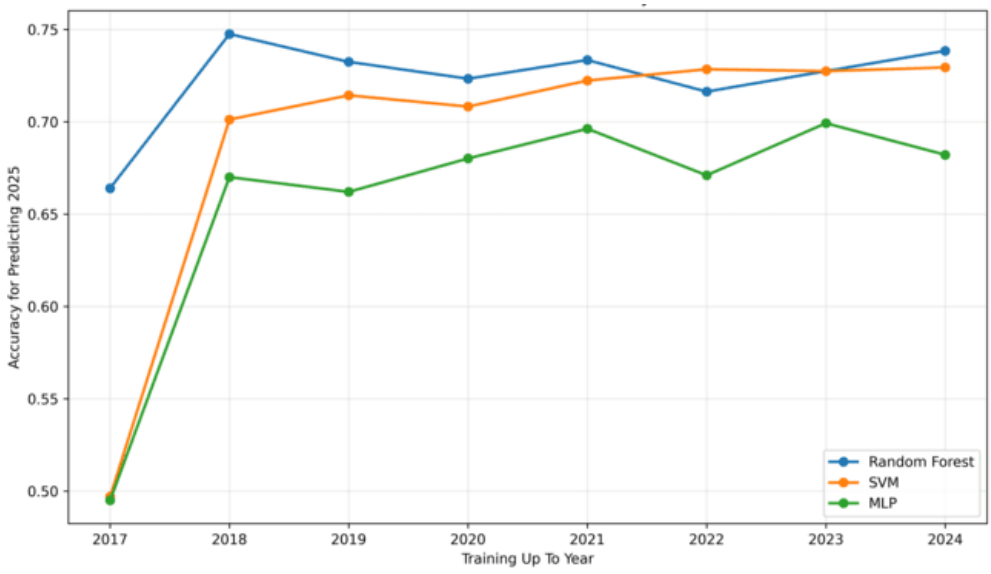

Figure 10: Accuracy of Cumulative Models (2017-2024) When Predicting Flood Conditions for 2025

Given RF's highest accuracy and lowest misclassification rate, the final RF model trained on 2017-2024 was selected to generate the 2025 binary flood prediction raster (Figure 10). The resulting spatial flood pattern shows strong alignment with historically inundated areas and observed flood-prone drainage corridors in the region, supporting the usability of the RF time-series ensemble for annual flood forecasting applications.

4.5. Spatial Prediction of Flood Occurrence for 2025

The trained binary flood prediction models (RF, SVM, MLP) were used to forecast the 2025 flood pattern using 2017-2024 hydro-meteorological inputs. All models produced inundation concentrated along river corridors and adjacent low-lying floodplains, indicating effective learning of terrain-controlled flood dynamics. Among them, Random Forest (RF) generated the most geomorphologically consistent map, showing coherent flood clusters aligned with the Panchganga River and smooth transitions into higher terrain. SVM produced sharper boundaries, reflecting strict margin-based decision surfaces (Mountrakis *et al.*, 2011), while MLP slightly over predicted inundation in agricultural and peri-urban zones due to sensitivity to soil moisture and land-cover heterogeneity (Pham *et al.*, 2020). These patterns reinforce RF's superior ability to capture realistic flow pathways and terrain-governed inundation behavior.

These spatial differences align with the quantitative performance metrics from the cumulative training windows. Random Forest (RF) achieved the highest accuracy (~73.84% in 2024), outperforming SVM (~72.94%) and MLP (~68.21%). Confusion-matrix evaluation on the independent 2025 dataset further confirmed RF's stronger generalization, indicated by higher true positives and substantially fewer false positives. This reflects RF's ability to distinguish flooded from non-flooded areas while avoiding the over prediction commonly reported in flood-susceptibility models (Choubin *et al.*, 2019; Khosravi *et al.*, 2018). In contrast, MLP produced elevated false-flood classifications, consistent with its spatial overestimation and sensitivity to heterogeneous hydrometeorological and land-surface conditions.

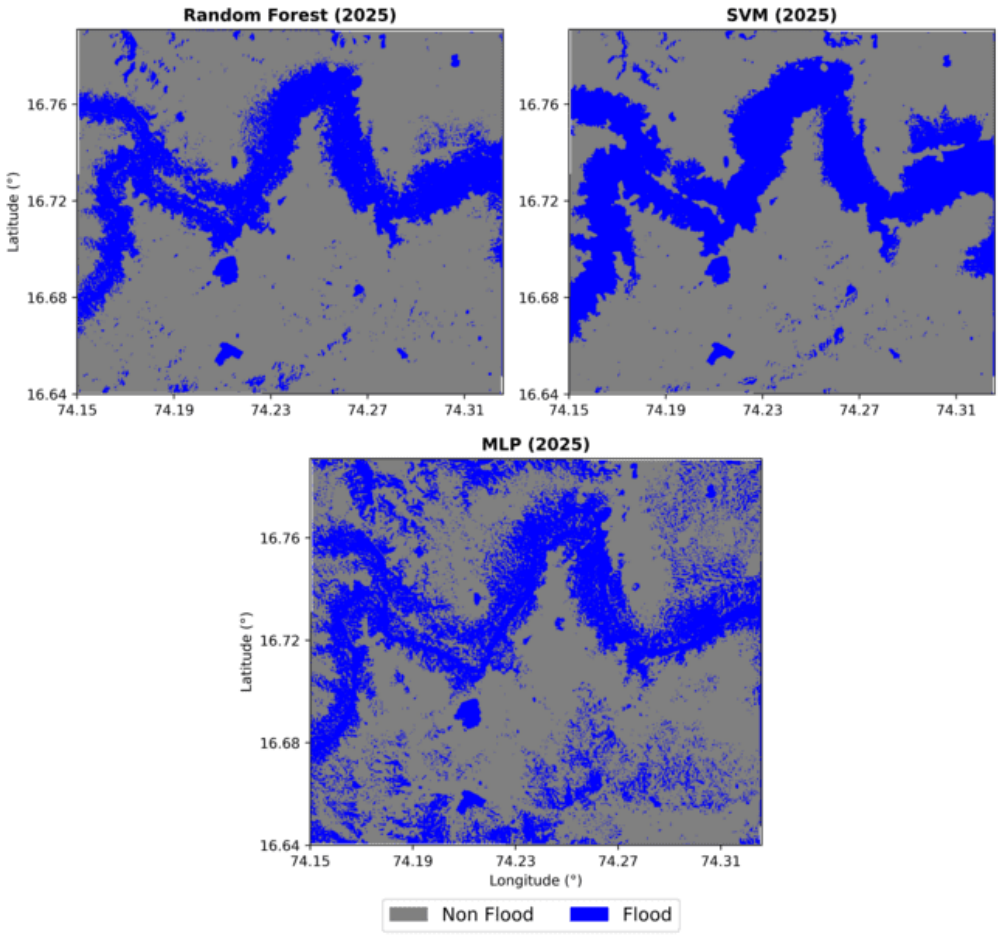

Figure 11: Machine Learning-Based Flood Inundation Predictions for 2025

4.6. Forecasting Capability of the 2017-2024 Trained Model

The cumulative accuracy assessment indicates that model performance improved as additional monsoon years were incorporated, demonstrating the value of training on diverse hydroclimatic conditions. The 2017-2024 configuration produced the highest internal accuracy and strongest transferability to 2025, consistent with findings that multi-year data improve representation of interannual variability in rainfall, antecedent wetness, and runoff—key controls on monsoon-driven flooding (Janizadeh *et al.*, 2019; Mosavi *et al.*, 2020; Khosravi *et al.*, 2018). Forecasting capability is supported by the model's use of rainfall and runoff predictors that become informative before inundation develops. The 15-day moving-average rainfall metric captures antecedent moisture and cumulative thresholds known to initiate flooding (IMD, 2022; Jain *et al.*, 2012), enabling advance susceptibility estimates. This aligns with hydrological theory identifying antecedent rainfall and catchment wetness as leading indicators (Sharma *et al.*, 2018; Rahmani *et al.*, 2019). Operationally, the framework supports short-range monsoon forecasting, with the 2017-2024 RF model providing a robust basis for anticipatory flood prediction in Kolhapur. Figure 11 shows Machine learning-based flood inundation predictions for 2025.

5. Transferability and Global Applicability

The modelling framework developed in this study is designed to extend beyond the Kolhapur basin and is broadly transferable to other monsoon-influenced and data-scarce river systems. Its generalizability arises from the use of globally accessible datasets—Sentinel-1 SAR imagery, CHIRPS and ERA5-Land hydrometeorological products, and SRTM terrain parameters—which are available at consistent spatial and temporal resolutions across most regions of the world. These datasets provide a standardized foundation for constructing flood–non-flood training archives even where in situ observations are limited or discontinuous.

The predictor suite used in the models—rainfall accumulation, runoff, elevation, slope, soil type, drainage density, and LULC—represents physical drivers of flood generation that are not unique to Kolhapur. Similar hydroclimatic and physiographic controls govern flood behavior in monsoon basins across South Asia, Southeast Asia, East Africa, and parts of South America. As such, the machine-learning framework can be directly adapted to these regions with minimal modification, provided sufficient SAR or rainfall-driven flood inventories are available.

The cumulative multi-year training approach further enhances transferability by capturing a wide spectrum of interannual monsoon variability, enabling the models to generalize across diverse rainfall patterns, antecedent wetness states, and hydrological extremes. This is particularly important for basins where climate variability or land-use change produces rapidly evolving flood dynamics.

Operationally, the workflow supports integration into early-warning systems because it relies on predictors—such as cumulative rainfall and runoff—that evolve prior to inundation. This allows application in basins where real-time river gauge data are sparse but where satellite rainfall and reanalysis data are routinely available. With minor calibration, the framework can also be extended to floodplain management, hotspot identification, and climate-sensitivity assessments in urbanizing river basins worldwide.

Overall, the methodological structure, predictor design, and reliance on open-access datasets make this workflow broadly applicable to global monsoon and riverine environments, addressing the need for transferable, data-driven flood forecasting tools in regions with limited hydrological monitoring infrastructure.

6. Conclusion

This study demonstrates that a multi-year, machine-learning framework integrating SAR, hydrometeorological data, and terrain attributes can reliably characterize and forecast monsoon-driven flooding in Kolhapur. The Random Forest classifier consistently outperformed SVM and MLP, producing spatially coherent inundation patterns and exhibiting strong generalization to the independently withheld 2025 flood event. Model performance improved progressively as additional monsoon seasons were incorporated, underscoring the value of long-term observational diversity for learning rainfall–runoff–inundation relationships under varying hydroclimatic conditions.

A key outcome of this work is the identification of antecedent hydrological indicators—particularly cumulative rainfall, runoff, and soil wetness—as effective predictors for short-range flood forecasting. These variables evolve prior to inundation and therefore provide actionable lead times for municipal response and early-warning systems.

Beyond the local case study, the workflow presented here offers substantial global applicability. Because it relies on open-access SAR observations, reanalysis-based hydrometeorological fields, and terrain-derived predictors, the methodology is readily transferable to other monsoon-affected and data-scarce river basins. The non-parametric nature of the machine-learning models further enables adaptation to heterogeneous physiographic and climatic settings with minimal structural modification.

Future enhancements—including higher-resolution rainfall inputs, assimilation of water-level observations, incorporation of dynamic soil-moisture products, and use of temporal deep-learning architectures—can further improve operational performance. Overall, this study provides a scalable, data-driven foundation for flood forecasting and risk management that can be extended to urban river systems across South Asia and other monsoon-regulated regions.

Acknowledgment

The authors express their sincere gratitude to Dr. Vidula Swami for her valuable guidance, technical insights, and continuous support throughout the course of this research. The authors also acknowledge Shivaji University, Kolhapur, for providing academic resources, institutional support, and an enabling research environment essential for completing this work.

Conflict of Interest

No potential conflict of interest.

Funding

No external funding or grant support was received for this study.

Data Availability Statement

The data will be made available upon reasonable request.

Disclosure Statement

The authors used OpenAI's ChatGPT (version 5.1) as a language-support tool for improving clarity, grammar, and structure of the manuscript. No AI tool was used to generate scientific ideas, data, content, analyses, interpretations, or conclusions. All AI-assisted text was reviewed, verified, and edited by the authors to ensure accuracy and integrity.

Author Contributions

Shrikant Kate: Conceptualization; methodology; data curation; formal analysis; investigation; software; visualization; writing—original draft; writing—review and editing; validation; project administration; resources.

Dr. Vidula Swami: Supervision; guidance; conceptual support; writing – review and editing; critical feedback; validation.

References

Abadi, M., Barham, P., Chen, J. *et al.* (2016). TensorFlow: A System for Large-Scale Machine Learning. *Proceedings of the 12th USENIX Symposium on Operating Systems Design and Implementation*, 265-283.

Amitrano, D., Guida, R., Iodice, A., Riccio, D. and Ruello, G. (2020). Flood Detection Using SAR Data and Digital Elevation Model Constraints. *Remote Sensing*, 12, 1048.

Bergstra, J. and Bengio, Y. (2012). Random Search for Hyper-Parameter Optimization. *Journal of Machine Learning Research*, 13, 281-305.

Breiman, L. (2001). Random Forests. *Mach. Learn.*, 45, 5-32. https://doi.org/10.1023/A:1010933404324

Central Ground Water Board (CGWB) (2019). Ground Water Information: Kolhapur District, Maharashtra. Western Region, Ministry of Jal Shakti, Government of India.

Choubin, B. *et al.* (2019). Ensemble Prediction of Flood Susceptibility Using RF and Decision Trees. *Sci. Total Environ.*, 651, 2087-2096. https://doi.org/10.1016/j.scitotenv.2018.10.032

Cortes, C. and Vapnik, V. (1995). Support-Vector Networks. *Mach. Learn.*, 20, 273-297. https://doi.org/10.1007/BF00994018

Dey, S., Jain, S.K. and Kumar, V. (2022). Hydrometeorological Controls on Monsoon Flooding in Indian River Basins. *J. Hydrol.*, 604, 127276. https://doi.org/10.1016/j.jhydrol.2021.127276

Funk, C., Peterson, P., Landsfeld, M. *et al.* (2015). The Climate Hazards Infrared Precipitation with Stations (CHIRPS) Dataset. *Scientific Data*, 2, 150066.

Gadgil, S. (2018). The Monsoon System: Land-Sea Breeze, ITCZ, ENSO and Monsoon Variability. *Curr. Sci.*, 114, 379-390.

Ganjirad, N. and Delavar, M.R. (2023). SAR-Based Flood Inventory Updating and Machine Learning-Driven Flood Susceptibility Modelling in Data-Scarce Regions. *Nat. Hazards*, 120, 1123-1145. https://doi.org/10.1007/s11069-023-06020-1

Ho, T. and Mostafavi, M. (2025). Patch-Level Flood Inundation Mapping Using Random Forest and Sentinel-1 SAR Data: Case Study of Tropical Storm Imelda. *Remote Sens.*, 17, 1869. https://doi.org/10.3390/rs17111869

Houze, R.A. Jr., McMurdie, L.A., Rasmussen, K.L., Kumar, V. and Chaplin, M.M. (2017). Monsoon Convection and Extreme Rainfall. *Rev. Geophys.*, 55, 486-518. https://doi.org/10.1002/2016RG000549

India Meteorological Department (IMD). (2022). Climate Profile of Maharashtra. IMD, Pune, India.

Iselborn, M., Kaya, S. and Eris, E. (2023). Machine-Learning-Based Flood Extent Mapping Using Sentinel-1/2 Imagery for the 2021 Gediz Plain Flood. *J. Hydrol.*, 617, 128921. https://doi.org/10.1016/j.jhydrol.2022.128921

Jain, S.K., Mani, P., Ojha, C.S.P. and Singh, V.P. (2021). Antecedent Rainfall Thresholds for Flood Generation in Indian River Basins. *Journal of Hydrology*, 598, 126429.

Jain, V.K., Tandon, S.K. and Sinha, R. (2018). Geomorphic Controls on Flood Risk in Monsoon Rivers. *Curr. Sci.*, 114, 567-575.

Janizadeh, S. *et al.* (2019). Flood Susceptibility Mapping Using Machine Learning Techniques. *J. Hydrol.*, 573, 311-323. https://doi.org/10.1016/j.jhydrol.2019.03.036

Khosravi, K. *et al.* (2018). Ensemble and Hybrid Machine Learning Models for Flood Susceptibility Assessment. *J. Hydrol.*, 564, 207-222. https://doi.org/10.1016/j.jhydrol.2018.07.008

Kumar, P., Avtar, R., Dasgupta, R., Johnson, B.A., Mukherjee, A., Ahsan, M.N., Nguyen, D.C.H. and Nguyen, H.Q., Shaw, R. and Mishra, B.K. (2020). Socio-Hydrology: A Key Approach for Adaptation to Water Scarcity and Achieving Human Well-Being in Large Riverine Islands. Progress in Disaster Science, 8,Article 100134. https://doi.org/10.1016/j.pdisas.2020.100134

Manfreda, S. *et al.* (2018). Remote Sensing in Flood Mapping and Monitoring: A Review. *Remote Sens.*, 10, 1836. https://doi.org/10.3390/rs10111836

Mosavi, A. *et al.* (2020). Remote Sensing and Machine Learning for Flood Forecasting: A Meta-Analysis. *Water Resour. Manag.*, 34, 4167-4186. https://doi.org/10.1007/s11269-020-02656-x

Mosavi, A., Ozturk, P. and Chau, K.-W. (2018). Flood Prediction Using Machine Learning Models: A Review. *Water*, 10, 1536. https://doi.org/10.3390/w10111536

Mountrakis, G., Im, J. and Ogole, C. (2011). Support Vector Machines in Remote Sensing: A Review. *ISPRS J. Photogramm. Remote Sens.*, 66, 247-259. https://doi.org/10.1016/j.isprsjprs.2010.11.001

Muñoz-Sabater, J., Dutra, E., Agustí-Panareda, A. *et al.* (2021). ERA5-Land: A State-of-the-Art Global Reanalysis Dataset. *Earth System Science Data*, 13, 4349-4383.

Pedregosa F. *et al.* (2011). Scikit-Learn: Machine Learning in Python. *J. Mach. Learn. Res.*, 12, 2825-2830.

Pham, H.T. *et al.* (2020). Sentinel-1 SAR for Flood Inundation Mapping in Monsoon Regions. *Hydrol. Earth Syst. Sci.*, 24, 577-593. https://doi.org/10.5194/hess-24-577-2020

Rahmani, V., Hutchinson, S.L. and Harrington, J. (2019). Antecedent Soil Moisture and Flood Prediction. *Water Resources Research*, 55, 1656-1673.

Rodríguez-Blanco, M.L., Taboada-Castro, M.M. and Taboada-Castro, M.T. (2012). Rainfall-Runoff Response in a Humid Agricultural Catchment. *Hydrol. Process.*, 26, 1478-1490. https://doi.org/10.1002/hyp.8281

Rumelhart, D.E., Hinton, G.E. and Williams, R.J. (1986). Learning Representations by Back-Propagating Errors. *Nature*, 323, 533-536. https://doi.org/10.1038/323533a0

Sanyal, J. and Lu, X.X. (2004). Application of Remote Sensing in Flood Management with Special Reference to Monsoon Asia. *Nat. Hazards*, 33, 283-301. https://doi.org/10.1023/B:NHAZ.0000037035.65105.95

Sharma, N., Ojha, C.S.P. and Singh, R. (2021). Rainfall Variability and Flood Response in Urban Monsoon Environments. *J. Hydrol. Eng.*, 26, 04021008. https://doi.org/10.1061/(ASCE)HE.1943-5584.0002067

Shen, X., Wang, D., Mao, K., Anagnostou, E. and Hong, Y. (2019). Inundation Mapping Using Sentinel-1 SAR Imagery. *Remote Sensing*, 11, 1174.

Singha, S. and Swain, K. (2022). Sentinel-1 SAR for Monsoon-Season Flood Detection in the Indo-Gangetic Plains. *Environ. Sci. Pollut. Res.*, 29, 65150-65163. https://doi.org/10.1007/s11356-022-20954-5

Taylor, K.E. (2001). Summarizing Multiple Aspects of Model Performance in a Single Diagram. *J. Geophys. Res.*, 106, 7183-7192. https://doi.org/10.1029/2000JD900719

Tehrany, M.S., Pradhan, B. and Jebur, M.N. (2014). Flood Susceptibility Mapping Using a Hybrid Ensemble Approach. *Stoch. Environ. Res. Risk Assess.*, 28, 2061-2076. https://doi.org/10.1007/s00477-014-0917-6

Twele, A., Cao, W., Plank, S. and Martinis, S. (2016). Sentinel-1-Based Flood Mapping. *Remote Sensing*, 8, 95.

Willmott, C.J., Robeson, S.M. and Matsuura, K. (2012). A Refined Index of Model Performance. *Int. J. Climatol.*, 32, 2088-2094. https://doi.org/10.1002/joc.2419

Cite this article as: Shrikant Kate and Vidula Swami (2026). Multi-Year Flood Inundation Modelling in Kolhapur, India Using SAR Observations and Machine Learning. *International Journal of Artificial Intelligence and Machine Learning*, 6(1), 102-117. doi: 10.51483/IJAIML.6.1.2026.102-117.